Heterotic mini-landscape (II): Completing the search for MSSM vacua in a $\mathbb{Z}_6$ orbifold

Oleg Lebedev [a], Hans Peter Nilles [b], Saúl Ramos-Sánchez [b,*], Michael Ratz [c], Patrick K.S. Vaudrevange [b]

[a] *CERN, Theory Division, CH-1211 Geneva 23, Switzerland*
[b] *Physikalisches Institut der Universität Bonn, Nussallee 12, 53115 Bonn, Germany*
[c] *Physik Department T30, Technische Universität München, James-Franck-Straße, 85748 Garching, Germany*

ABSTRACT

We complete our search for MSSM vacua in the $\mathbb{Z}_6$-II heterotic orbifold by including models with 3 Wilson lines. We estimate the total number of inequivalent models in this orbifold to be 10^7. Out of these, we find almost 300 models with the exact MSSM spectrum, gauge coupling unification and a heavy top quark. Models with these features originate predominantly from local GUTs. The scale of gaugino condensation in the hidden sector is correlated with properties of the observable sector such that soft masses in the TeV range are preferred.

1. Introduction

Construction of the (supersymmetric) standard model vacua has been one of the top priorities in string theory. Although there is a vast landscape of string theory vacua [1,2], realistic models are extremely rare. For example, in Gepner models the probability of finding a model with the massless spectrum of the minimal supersymmetric standard model (MSSM) plus vector-like exotics is of order 10^{-14} [3] while this probability in $\mathbb{Z}_6$ intersecting brane models is 10^{-16} [4] (for models with chiral exotics it is 10^{-9} [5]). The heterotic string [6–14], on the other hand, provides a more fertile ground for realistic constructions due to its built-in grand unification structures. In particular, there are fertile regions in the $\mathbb{Z}_6$-II heterotic orbifold with 2 Wilson lines where the probability of finding a model with the *exact* MSSM spectrum is somewhat below 1% [15] and about 100 such models have been identified (see also [16–20]). In this Letter, we complete our search [15] within the $\mathbb{Z}_6$-II heterotic orbifold by including models with 3 Wilson lines, which is the maximal possible number of Wilson lines in the $\mathbb{Z}_6$-II orbifold. This allows us to estimate the total number of inequivalent models in this orbifold and construct further examples of MSSMs. Unlike in the presence of 2 Wilson lines, all 3 matter generations are fundamentally different in this case.

In the first part of our analysis, we consider the gauge shifts associated with SO(10) or E_6 local grand unified theories (GUTs). This is the strategy we have pursued in our previous paper [15]. Inspired by an orbifold GUT interpretation of heterotic models [21–24], *local GUTs* [24–28] are specific to certain points in the

compact space such that twisted states localized at these points form complete representations of the corresponding GUT group. On the other hand, the 4D gauge symmetry is that of the SM and the bulk states such as gauge bosons (and Higgs doublets) only form representations of the latter. This provides a heuristic explanation of the apparent GUT structure of the SM matter multiplets without having a 4D GUT. The MSSM search strategy based on local GUT gauge shifts has been very successful and led to identification of about 100 models with the exact MSSM spectrum [15]. All these models involve 2 Wilson lines and share the common feature that 2 matter generations are very similar, while the third one is fundamentally different. They all have the top quark Yukawa coupling of order one and are consistent with gauge coupling unification. In our current work, we extend these results to models with 3 Wilson lines and construct further $\mathcal{O}(100)$ models with the MSSM spectrum. In this case, all 3 matter generations are different which leads to distinct (but not necessarily "healthier") phenomenology.

In the second part of our analysis, we relax the requirement of having SO(10) or E_6 local GUTs and construct MSSMs based on arbitrary gauge shifts. This is interesting as it allows us to determine how likely is a given model with the MSSM spectrum to have originated from a local GUT. Finally, we provide a representative example of a 3 WL model with the exact MSSM spectrum.

2. Constructing MSSMs

In our previous mini-landscape study [15], we have analyzed models with up to 2 Wilson lines and local SO(10) and E_6 structures. Let us briefly review the key ingredients of this construction (for more details, see [26,29]). An orbifold model is defined by the orbifold twist, the torus lattice and the gauge embedding of the

* Corresponding author.
E-mail address: ramos@th.physik.uni-bonn.de (S. Ramos-Sánchez).

Table 1

Statistics of $\mathbb{Z}_6$-II orbifold models based on the shifts $V^{SO(10),1}$, $V^{SO(10),2}$, $V^{E_6,1}$, $V^{E_6,2}$ with three non-trivial Wilson lines

Criterion	$V^{SO(10),1}$	$V^{SO(10),2}$	$V^{E_6,1}$	$V^{E_6,2}$
(2) ineq. models with 3 WL	942,469	246,779	8815	37,407
(3) SU(3) × SU(2) gauge group	373,412	89,910	2321	13,857
(4) 3 net (**3, 2**)	5853	2535	352	745
(5) non-anomalous $U(1)_Y \subset SU(5)$	2620	1294	314	420
(6) spectrum = 3 generations + vectorlike	45	19	123	0
(7) heavy top	44	1	123	0
(8) exotics decouple at order 8	20	1	60	0

orbifold action, i.e. the gauge shift V and the Wilson lines W_n. The $\mathbb{Z}_6$-II orbifold allows us to switch on one Wilson line of degree 3 (W_3) and up to two of degree 2 (W_2 and W_2'). A given V corresponds to the SO(10) or E_6 local GUT if the left-moving momenta p satisfying

$$p \cdot V = 0 \bmod 1, \qquad p^2 = 2, \tag{1}$$

are roots of SO(10) or E_6 (up to extra gauge factors). In addition, this V must allow for massless **16**-plets of SO(10) at the fixed points with SO(10) symmetry or **27**-plets of E_6 at the fixed points with E_6 symmetry. Since massless states from T_1 are automatically invariant under the orbifold action, they all survive in 4D and appear as complete GUT multiplets. In the case of SO(10), that gives one complete SM generation, while in the case of E_6 it is necessary to decouple part of the **27**-plet since **27** = **16** + **10** + **1** under SO(10). Then, choosing appropriate Wilson lines W_n, one obtains the SM gauge group in 4D. Furthermore, in order to have the correct hypercharge normalization, one requires the embedding $G_{SM} \subset SU(5)$.

In the $\mathbb{Z}_6$-II orbifold, there are 2 gauge shifts leading to a local SO(10) GUT,

$$V^{SO(10),1} = \left(\tfrac{1}{3}, \tfrac{1}{2}, \tfrac{1}{2}, 0, 0, 0, 0, 0\right) \left(\tfrac{1}{3}, 0, 0, 0, 0, 0, 0, 0\right),$$

$$V^{SO(10),2} = \left(\tfrac{1}{3}, \tfrac{1}{3}, \tfrac{1}{3}, 0, 0, 0, 0, 0\right) \left(\tfrac{1}{6}, \tfrac{1}{6}, 0, 0, 0, 0, 0, 0\right), \tag{2}$$

and 2 shifts leading to a local E_6 GUT,

$$V^{E_6,1} = \left(\tfrac{1}{2}, \tfrac{1}{3}, \tfrac{1}{6}, 0, 0, 0, 0, 0\right) \left(0, 0, 0, 0, 0, 0, 0, 0\right),$$

$$V^{E_6,2} = \left(\tfrac{2}{3}, \tfrac{1}{3}, \tfrac{1}{3}, 0, 0, 0, 0, 0\right) \left(\tfrac{1}{6}, \tfrac{1}{6}, 0, 0, 0, 0, 0, 0\right). \tag{3}$$

Having fixed these shifts, one scans over possible Wilson lines to get the SM gauge group. To identify MSSM candidates, we have taken the following steps:

Step 1. Generate Wilson lines W_3 and W_2;
Step 2. Identify "inequivalent" models;
Step 3. Select models with $G_{SM} \subset SU(5) \subset SO(10)$ or E_6;
Step 4. Select models with three net (**3, 2**);
Step 5. Select models with non-anomalous $U(1)_Y \subset SU(5)$;
Step 6. Select models with net 3 SM families + Higgses + vectorlike exotics;
Step 7. Select models with a heavy top;
Step 8. Select models in which the exotics decouple.

The result was that out of 3×10^4 inequivalent models about 100 models satisfied our MSSM-requirements. Thus, close to 1% of all models were acceptable. These models have 2 identical matter generations from two localized **16**- or **27**-plets, which is due to the presence of one Wilson line of order three (W_3) and one Wilson line of order two (W_2).

In this Letter, we extend our previous analysis by allowing for 3 Wilson lines, which is the maximal possible number of Wilson lines in the $\mathbb{Z}_6$-II orbifold. An immediate consequence of this is that all three matter generations obtained in this case would have a different composition. Also, since (due to combinatorics) most

models in the $\mathbb{Z}_6$-II orbifold have 3 Wilson lines, this allows us to estimate the total number of all possible models and the probability of finding the MSSM by a "blind scan". Furthermore, we relax the requirement of the hypercharge embedding into a local SO(10) or E_6 GUT, while still having the correct GUT hypercharge normalization. Finally, we drop the requirement of having a local SO(10) or E_6 GUT. Besides constructing new models, all this helps us understand whether (and how) the "intelligent" search strategy based on local GUTs is more efficient than a "blind scan". Also, given a model with the exact MSSM spectrum, gauge coupling unification and a heavy top quark, we can determine how likely it is to have come from a local GUT.

2.1. 3 WL models with local GUTs

We start by studying the models with local GUT shifts of [15]. Our results are presented in Table 1. Note the difference in Step 3 compared to that in the 2 Wilson line case: now we do not require the hypercharge embedding in SU(5) ⊂ SO(10) at this step, whereas at Step 5 we require $U(1)_Y \subset SU(5)$ with SU(5) not necessarily being inside SO(10) (or E_6). This allows us to retain more models while keeping the standard GUT hypercharge normalization.

Compared to the 2 WL case, the total number of inequivalent models has grown from 3×10^4 to 10^6. In the end, however, we retain only about 100 new models.[1] Thus the efficiency is much lower than that in the 2 WL case. It is interesting that most of the models at Step 8 come form the E_6 local GUT with the gauge shift $V^{E_6,1}$. The fact that E_6 models contribute much more in the 3 WL than 2 WL case is understood by symmetry breaking: it is easier to get to the SM gauge group from E_6 using 3 Wilson lines.

A comment is in order. Due to our computing limitations, we define two models to be "equivalent" if they have identical non-Abelian massless spectra and the same number of non-Abelian massless singlets. This does not take into account the possibility that the singlets can have different U(1) charges, nor that fields with identical gauge quantum numbers can differ in their localization, etc. These differences can sometimes be important, for example, for the decoupling of exotics since the relevant mass terms can be allowed in one case and not the other. As a result, we underestimate the number of inequivalent models. The resulting uncertainty in our numbers is found empirically to be within a factor of 2.

2.2. A statistical analysis of general 3 WL models

Now we turn to the discussion of general 3 WL models, i.e. we no longer demand that there is a local SO(10) or E_6. The number of models with 3 Wilson lines is very large and, unlike in the case of 2 Wilson lines, constructing all of them (in the sense of calculating the spectrum) is an extremely time-consuming task. The reason is that the known ways of constructing all inequivalent models lead to huge redundancies because different shifts and

---

[1] The models with the exact MSSM spectrum are listed in [30].

Wilson lines can be related by elements of the Weyl group (cf. the discussion in [31]). Thus, it becomes impossible to check how many of them are equivalent. Instead of the complete classification of models we use a statistical approach (for related discussion see [32–34]). To understand the basic idea, consider a simple example. Suppose we have a set of M models out of which N are inequivalent ($M, N \gg 1$). Assume also that each inequivalent model is represented M/N times in the set M, which corresponds a "flat distribution". The probability that 2 randomly chosen models are equivalent is $1/N$. Take now a larger random selection of models n, $1 \ll n \ll N$. The probability that there are equivalent models in this set is

$$p(n, N) \simeq \binom{n}{2} \frac{1}{N} \simeq \frac{n^2}{2N}. \tag{4}$$

For $n = \sqrt{N}$, this probability is $1/2$. Thus, in a sample of $\sqrt{N}$ out of a total of N models, there is order 1 probability that at least 1 model is redundant. This observation allows us to estimate the number of inequivalent models by studying a sample of order $\sqrt{N}$ models.

As the first step, we use the following simple algorithm. Start with a random model. Then generate another model and compare it to the first one. If they are equivalent, stop the procedure. Otherwise, generate another model and compare it to the previous ones, and so on. The probability that this procedure terminates at a sample of size n is

$$P(n, N) = \frac{n}{N} \prod_{k=1}^{n-1} \left(1 - \frac{k}{N}\right). \tag{5}$$

The maximum of this function is at $n = \sqrt{N}$. Thus, if we produce a number of sets of models with different n and plot how common a particular n is, the maximum of this distribution should give $n = \sqrt{N}$.

An important assumption in this analysis is that all inequivalent models are equally likely to be generated. In practice, this is not the case and some models appear more often than the others. This, in particular, has to do with the specifics of the model-generating routine. To take this factor into account, we introduce a fudge parameter t defined by $nt \simeq \sqrt{N}$, where n is the predominant size of the sample (as defined above) and N is the true number of inequivalent models. The parameter t can be determined "experimentally" when both n and N are known, for example, from the 2 Wilson line case distributions or subsets of 3 Wilson line case distributions. We find a rather stable value $t \simeq 2$ independently of the sample considered and adopt this value for the rest of our analysis.

Using these methods, we consider models with all possible gauge shifts, and 2 and 3 non-trivial Wilson lines. We find that there are about 10^7 inequivalent models. Out of these, we have constructed explicitly all possible models with 2 WLs and a sample of 5×10^6 models with 3 WLs. This resulted in 267 MSSMs.[2] Most of them originate from E_6, SO(10) and SU(5) local GUTs as shown in Table 2. Note that models with SU(5) local structure do not have a complete localized family, rather only part of it. The additional states come from other sectors of the model. The conclusion is that any model with the exact MSSM spectrum, gauge coupling unification and a heavy top quark is likely to have come from some local GUT.

An important characteristic of MSSM candidates is the size of the hidden sector which determines the scale of gaugino conden-
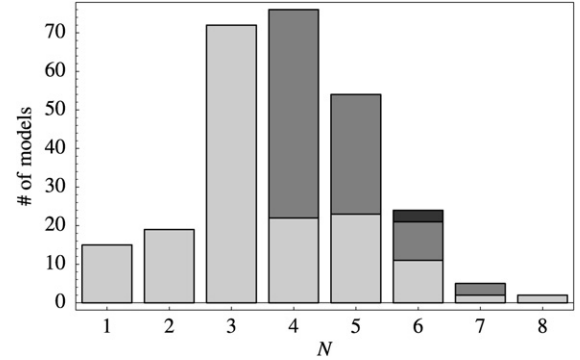
Table 2
Local GUT structure of the MSSM candidates. These gauge groups appear at some fixed point(s) in the T_1 twisted sector. The SU(5) local GUT does not produce a complete family, so additional "non-GUT" states are required

Local GUT	"family"	2 WL	3 WL
E_6	**27**	14	53
SO(10)	**16**	87	7
SU(6)	**$15 + \bar{6}$**	2	4
SU(5)	**10**	51	10
Rest		39	0
Total		193	74
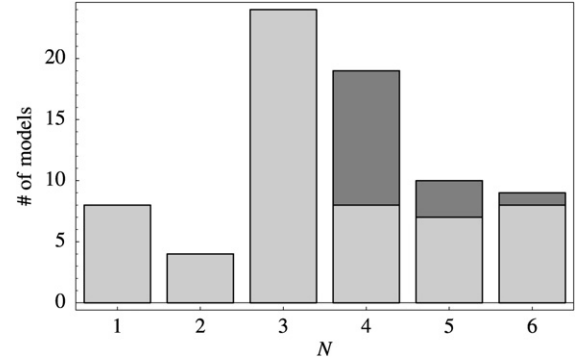
Fig. 1. Number of MSSM candidates vs. largest gauge group in the hidden sector. SU(N)/SO($2N$)/E_N are given by light/dark/darker bins. (a): models with 3 WL, (b): models with 2 and 3 WL.

sation Λ and consequently the scale of soft SUSY breaking masses $m_{3/2}$ [35–38],

$$m_{3/2} \sim \frac{\Lambda^3}{M_P^2}, \tag{6}$$

where M_P denotes the Planck scale. If the largest hidden sector gauge factor is too big, e.g. E_6 or E_8, the gaugino condensation scale is too high and supersymmetry is irrelevant to low energy physics. If it is too low, the model is ruled out by experiment. It is intriguing that, in the 2 WL case, most of the MSSM-candidates automatically have the gaugino condensation scale in the right ballpark, that is around 10^{12}–10^{13} GeV [39]. For 3 Wilson lines, we present the statistics of the hidden sector gauge groups in Fig. 1(a). There N labels the "size" of the gauge groups SU(N) and SO($2N$). Although the peak of this distribution is at $N = 3$ corresponding to SU(3), a significant fraction of the models have $N = 4, 5$ which leads (in the absence of hidden matter) to gaugino condensation at an intermediate scale. If SUSY breaking is due to gaugino con-

---

[2] Here we only obtain 74 MSSMs with 3 WL which is fewer than the number in Table 1. This is because our sample of 5×10^6 models does not contain all models with local SO(10) and E_6.

densation, the corresponding soft masses are in the TeV range as favored by phenomenology.

Combining both 2 and 3 WL models, we get a distribution peaking at $N = 4$ (Fig. 1(b)). The corresponding gaugino condensation scales are plotted in Fig. 2. It is remarkable that requiring the exact MSSM spectrum in the observable sector constrains the hidden sector such that gaugino condensation at an intermediate scale is automatically preferred. This provides a top-down motivation for TeV scales in particle physics.

2.3. Example

The model is defined by the gauge shift and Wilson lines

$$V^{E_6,1} = \left(\tfrac{1}{2}, \tfrac{1}{3}, \tfrac{1}{6}, 0, 0, 0, 0, 0\right) (0, 0, 0, 0, 0, 0, 0, 0), \tag{7a}$$

$$W_2 = \left(-\tfrac{1}{2}, 1, -\tfrac{1}{2}, -1, 0, 0, -\tfrac{1}{2}, -\tfrac{1}{2}\right)$$
$$\times \left(-\tfrac{3}{4}, -\tfrac{1}{4}, -\tfrac{1}{4}, -\tfrac{1}{4}, -\tfrac{1}{4}, \tfrac{1}{4}, \tfrac{1}{4}, \tfrac{1}{4}\right), \tag{7b}$$

$$W_2' = \left(\tfrac{1}{4}, -\tfrac{1}{4}, -\tfrac{1}{4}, -\tfrac{7}{4}, \tfrac{1}{4}, -\tfrac{3}{4}, \tfrac{1}{4}, \tfrac{5}{4}\right)$$
$$\times \left(0, -1, \tfrac{1}{2}, \tfrac{1}{2}, 1, 0, 1, 1\right), \tag{7c}$$

$$W_3 = \left(-\tfrac{1}{6}, \tfrac{1}{2}, -\tfrac{1}{2}, \tfrac{5}{6}, -\tfrac{1}{6}, -\tfrac{1}{6}, -\tfrac{1}{6}, -\tfrac{1}{6}\right)$$
$$\times \left(\tfrac{2}{3}, -1, 0, 0, 0, -\tfrac{1}{3}, 0, \tfrac{2}{3}\right). \tag{7d}$$

It has an E_6 local GUT at the origin of the torus lattice. The gauge group after compactification is

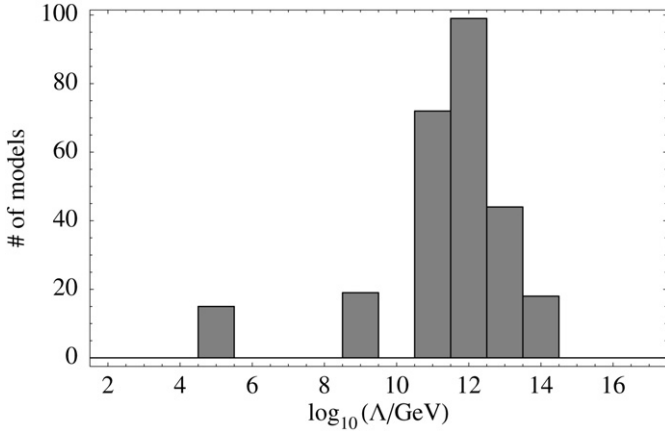$$G_{SM} \times [SU(3) \times SU(5)] \times U(1)^6, \tag{8}$$

Fig. 2. Number of MSSM candidates with 2 and 3 Wilson lines vs. the scale of gaugino condensation.

where $G_{SM} = SU(3)_C \times SU(2)_L \times U(1)_Y$ includes the standard SU(5) hypercharge generator

$$t_Y = \left(0, 0, 0, \tfrac{1}{3}, \tfrac{1}{3}, \tfrac{1}{3}, -\tfrac{1}{2}, -\tfrac{1}{2}\right) (0, 0, 0, 0, 0, 0, 0, 0). \tag{9}$$

The resulting massless spectrum is displayed in Table 3. One of the SM families comes from the **27**-plet of E_6 at the origin, while the other two come from various twisted and untwisted sectors. All three generations are intrinsically different in this model.

At this stage, the model has three generations of SM matter plus vector-like exotics. Once the SM singlets $s_i = \{s_i^0, h_i, \bar{h}_i\}$ develop nonzero VEVs, the gauge group breaks to

$$G_{SM} \times G_{hidden} \tag{10}$$

with $G_{hidden} = SU(5)$. Furthermore, we have verified that the mass matrices of the vector-like exotics have maximal rank. Therefore, all the exotics decouple from the low energy theory. These mass matrices are given by

$$\mathcal{M}_{\ell\bar\ell} = \begin{pmatrix}
s^3 & s^1 & s^1 & s^5 & s^5 & s^5 & s^5 & s^1 & s^1 & s^2 \\
s^1 & s^5 & s^5 & 0 & 0 & 0 & 0 & s^3 & s^3 & s^3 \\
s^3 & s^4 & s^4 & s^4 & s^5 & s^5 & s^5 & s^1 & s^1 & s^2 \\
s^3 & s^4 & s^4 & s^5 & s^4 & s^5 & s^5 & s^1 & s^1 & s^2 \\
s^3 & s^4 & s^4 & s^5 & s^5 & s^4 & s^5 & s^1 & s^1 & s^2 \\
s^3 & s^4 & s^4 & s^5 & s^5 & s^5 & s^4 & s^1 & s^1 & s^2 \\
s^3 & s^4 & s^4 & s^4 & s^5 & s^5 & s^5 & s^1 & s^1 & s^2 \\
s^3 & s^4 & s^4 & s^5 & s^4 & s^5 & s^5 & s^1 & s^1 & s^2 \\
s^3 & s^4 & s^4 & s^5 & s^5 & s^4 & s^5 & s^1 & s^1 & s^2 \\
s^3 & s^4 & s^4 & s^5 & s^5 & s^5 & s^4 & s^1 & s^1 & s^2 \\
s^1 & s^3 & s^3 & s^6 & s^6 & s^6 & s^6 & s^4 & s^4 & s^3 \\
s^4 & s^1 & s^1 & s^4 & s^6 & s^5 & s^5 & s^3 & s^3 & s^4 \\
s^4 & s^1 & s^1 & s^6 & s^4 & s^5 & s^5 & s^3 & s^3 & s^4 \\
s^4 & s^1 & s^1 & s^5 & s^5 & s^4 & s^6 & s^3 & s^3 & s^4 \\
s^4 & s^1 & s^1 & s^5 & s^5 & s^6 & s^4 & s^3 & s^3 & s^4
\end{pmatrix},$$

$$\mathcal{M}_{d\bar d} = \begin{pmatrix}
s^4 & s^4 & s^5 & s^5 & s^5 & s^5 & s^3 & s^3 & s^3 \\
s^4 & s^4 & s^4 & s^5 & s^5 & s^5 & s^1 & s^1 & s^2 \\
s^4 & s^4 & s^5 & s^4 & s^5 & s^5 & s^1 & s^1 & s^2 \\
s^4 & s^4 & s^5 & s^5 & s^4 & s^5 & s^1 & s^1 & s^2 \\
s^4 & s^4 & s^5 & s^5 & s^5 & s^4 & s^1 & s^1 & s^2 \\
s^4 & s^4 & s^4 & s^5 & s^5 & s^5 & s^1 & s^1 & s^2 \\
s^4 & s^4 & s^5 & s^4 & s^5 & s^5 & s^1 & s^1 & s^2 \\
s^4 & s^4 & s^5 & s^5 & s^4 & s^5 & s^1 & s^1 & s^2 \\
s^4 & s^4 & s^5 & s^5 & s^5 & s^4 & s^1 & s^1 & s^2 \\
s^3 & s^3 & s^6 & s^6 & s^6 & s^6 & s^4 & s^4 & s^2 \\
s^1 & s^1 & s^4 & s^6 & s^5 & s^5 & s^3 & s^3 & s^4 \\
s^1 & s^1 & s^6 & s^4 & s^5 & s^5 & s^3 & s^3 & s^4 \\
s^1 & s^1 & s^5 & s^5 & s^4 & s^6 & s^3 & s^3 & s^4 \\
s^1 & s^1 & s^5 & s^5 & s^6 & s^4 & s^3 & s^3 & s^4
\end{pmatrix},$$

Table 3
Massless spectrum. Representations with respect to $[SU(3)_C \times SU(2)_L] \times [SU(3) \times SU(5)]$ are given in bold face, the hypercharge is indicated by the subscript

#	Irrep	Label	#	Anti-irrep	Label	#	Irrep	Label
4	$(\mathbf{3},\mathbf{2};\mathbf{1},\mathbf{1})_{1/6}$	q_i	1	$(\mathbf{3},\mathbf{2};\mathbf{1},\mathbf{1})_{1/6}$	$\bar q_i$	26	$(\mathbf{1},\mathbf{1};\mathbf{1},\mathbf{1})_{0}$	s_i^0
14	$(\mathbf{1},\mathbf{2};\mathbf{1},\mathbf{1})_{-1/2}$	ℓ_i	8	$(\mathbf{1},\mathbf{2};\mathbf{1},\mathbf{1})_{1/2}$	$\bar\ell_i$	10	$(\mathbf{1},\mathbf{1};\bar{\mathbf{3}},\mathbf{1})_{0}$	$\bar h_i$
1	$(\mathbf{1},\mathbf{2};\bar{\mathbf{3}},\mathbf{1})_{-1/2}$	ℓ_i'	2	$(\mathbf{1},\mathbf{2};\mathbf{3},\mathbf{1})_{1/2}$	$\bar\ell_i'$	5	$(\mathbf{1},\mathbf{1};\mathbf{3},\mathbf{1})_{0}$	h_i
4	$(\bar{\mathbf{3}},\mathbf{1};\mathbf{1},\mathbf{1})_{-2/3}$	$\bar u_i$	1	$(\mathbf{3},\mathbf{1};\mathbf{1},\mathbf{1})_{2/3}$	u_i	1	$(\mathbf{1},\mathbf{1};\mathbf{1},\mathbf{5})_{0}$	w_i
4	$(\mathbf{1},\mathbf{1};\mathbf{1},\mathbf{1})_{1}$	$\bar e_i$	1	$(\mathbf{1},\mathbf{1};\mathbf{1},\mathbf{1})_{-1}$	e_i	1	$(\mathbf{1},\mathbf{1};\mathbf{1},\bar{\mathbf{5}})_{0}$	$\bar w_i$
13	$(\bar{\mathbf{3}},\mathbf{1};\mathbf{1},\mathbf{1})_{1/3}$	$\bar d_i$	7	$(\mathbf{3},\mathbf{1};\mathbf{1},\mathbf{1})_{-1/3}$	d_i			
1	$(\bar{\mathbf{3}},\mathbf{1};\bar{\mathbf{3}},\mathbf{1})_{1/3}$	$\bar d_i'$	2	$(\mathbf{3},\mathbf{1};\mathbf{3},\mathbf{1})_{-1/3}$	d_i'			
2	$(\mathbf{3},\mathbf{1};\mathbf{1},\mathbf{1})_{1/6}$	v_i	2	$(\bar{\mathbf{3}},\mathbf{1};\mathbf{1},\mathbf{1})_{-1/6}$	$\bar v_i$			
2	$(\mathbf{1},\mathbf{1};\mathbf{3},\mathbf{1})_{1/2}$	$\bar s_i^+$	2	$(\mathbf{1},\mathbf{1};\bar{\mathbf{3}},\mathbf{1})_{-1/2}$	$\bar s_i^-$			
8	$(\mathbf{1},\mathbf{1};\mathbf{1},\mathbf{1})_{1/2}$	s_i^+	8	$(\mathbf{1},\mathbf{1};\mathbf{1},\mathbf{1})_{-1/2}$	s_i^-			
4	$(\mathbf{1},\mathbf{2};\mathbf{1},\mathbf{1})_{0}$	m_i						

$$\mathcal{M}_{s^+s^-} = \begin{pmatrix} s^4 & s^5 & s^4 & s^4 & s^5 & s^6 & s^5 & s^5 & s^4 & s^5 \\ s^5 & s^4 & s^4 & s^4 & s^5 & s^4 & s^5 & s^5 & s^6 & s^5 \\ s^5 & s^5 & s^6 & s^6 & s^1 & s^6 & s^5 & s^6 & s^6 & s^6 \\ s^5 & s^5 & s^6 & s^6 & s^6 & s^4 & s^4 & s^6 & s^4 & s^4 \\ s^5 & s^5 & s^6 & 0 & s^4 & s^6 & s^3 & s^4 & s^6 & s^4 \\ s^5 & s^5 & s^6 & s^6 & s^6 & s^6 & s^6 & s^1 & s^6 & s^5 \\ s^5 & s^5 & s^6 & s^6 & s^6 & s^4 & s^4 & s^6 & s^4 & s^4 \\ s^5 & s^5 & 0 & s^6 & s^4 & s^6 & s^4 & s^4 & s^6 & s^3 \\ s^4 & s^4 & s^4 & s^6 & 0 & 0 & s^6 & s^6 & 0 & s^6 \\ s^4 & s^4 & s^6 & s^4 & s^6 & 0 & s^6 & 0 & 0 & s^6 \end{pmatrix},$$

$$\mathcal{M}_{q\bar{q}} = (\,s^3 \quad s^3 \quad s^3 \quad s^2\,),$$

$$\mathcal{M}_{u\bar{u}} = (\,s^4 \quad s^3 \quad s^3 \quad s^3\,),$$

$$\mathcal{M}_{e\bar{e}} = (\,s^4 \quad s^3 \quad s^3 \quad s^3\,),$$

$$\mathcal{M}_{v\bar{v}} = \begin{pmatrix} s^5 & s^6 \\ s^6 & s^5 \end{pmatrix},$$

$$\mathcal{M}_{mm} = \begin{pmatrix} 0 & s^6 & s^5 & s^4 \\ s^6 & 0 & s^4 & s^5 \\ s^5 & s^4 & 0 & s^6 \\ s^4 & s^5 & s^6 & 0 \end{pmatrix},$$

where ℓ collectively refers to ℓ_i and ℓ'_i, etc. At the same time, the hidden sector **5**-plets acquire large masses and decouple.

We note that the model allows for an order one top Yukawa coupling. It results from the couplings of the type *UUU* and *UTT*. Also, in this model, one can define a non-anomalous $B-L$ symmetry which gives standard charges for the SM matter. This feature is desired for proton stability, see [15,26,40,41].

3. Conclusions

We have completed our search for MSSMs in the $\mathbb{Z}_6$-II orbifold by including models with 3 Wilson lines. Out of a total of 10^7, we have identified almost 300 inequivalent models with the exact MSSM spectrum, gauge coupling unification and a heavy top quark. Models with these features originate predominantly from SO(10), E_6 and SU(5) local GUTs. Therefore, local GUTs are instrumental in obtaining the right models. We also find that the scale of gaugino condensation in the hidden sector is correlated with properties of the observable sector such that soft masses in the TeV range are preferred.

References

[1] W. Lerche, D. Lüst, A.N. Schellekens, Nucl. Phys. B 287 (1987) 477.
[2] L. Susskind, hep-th/0302219.
[3] T.P.T. Dijkstra, L.R. Huiszoon, A.N. Schellekens, Nucl. Phys. B 710 (2005) 3, hep-th/0411129.
[4] F. Gmeiner, G. Honecker, JHEP 0709 (2007) 128, arXiv: 0708.2285 [hep-th].
[5] F. Gmeiner, R. Blumenhagen, G. Honecker, D. Lüst, T. Weigand, JHEP 0601 (2006) 004, hep-th/0510170.
[6] D.J. Gross, J.A. Harvey, E.J. Martinec, R. Rohm, Phys. Rev. Lett. 54 (1985) 502.
[7] D.J. Gross, J.A. Harvey, E.J. Martinec, R. Rohm, Nucl. Phys. B 256 (1985) 253.
[8] L.J. Dixon, J.A. Harvey, C. Vafa, E. Witten, Nucl. Phys. B 261 (1985) 678.
[9] L.J. Dixon, J.A. Harvey, C. Vafa, E. Witten, Nucl. Phys. B 274 (1986) 285.
[10] L.E. Ibáñez, H.P. Nilles, F. Quevedo, Phys. Lett. B 187 (1987) 25.
[11] L.E. Ibáñez, H.P. Nilles, F. Quevedo, Phys. Lett. B 192 (1987) 332.
[12] L.E. Ibáñez, J.E. Kim, H.P. Nilles, F. Quevedo, Phys. Lett. B 191 (1987) 282.
[13] J.A. Casas, C. Muñoz, Phys. Lett. B 214 (1988) 63.
[14] J.A. Casas, E.K. Katehou, C. Muñoz, Nucl. Phys. B 317 (1989) 171.
[15] O. Lebedev, H.P. Nilles, S. Raby, S. Ramos-Sánchez, M. Ratz, P.K.S. Vaudrevange, A. Wingerter, Phys. Lett. B 645 (2007) 88, hep-th/0611095.
[16] V. Bouchard, R. Donagi, Phys. Lett. B 633 (2006) 783, hep-th/0512149.
[17] V. Braun, Y.-H. He, B.A. Ovrut, T. Pantev, JHEP 0605 (2006) 043, hep-th/0512177.
[18] R. Blumenhagen, S. Moster, T. Weigand, Nucl. Phys. B 751 (2006) 186, hep-th/0603015.
[19] J.E. Kim, B. Kyae, hep-th/0608085.
[20] J.E. Kim, J.-H. Kim, B. Kyae, JHEP 0706 (2007) 034, hep-ph/0702278.
[21] T. Kobayashi, S. Raby, R.-J. Zhang, Phys. Lett. B 593 (2004) 262, hep-ph/0403065.
[22] S. Förste, H.P. Nilles, P.K.S. Vaudrevange, A. Wingerter, Phys. Rev. D 70 (2004) 106008, hep-th/0406208.
[23] T. Kobayashi, S. Raby, R.-J. Zhang, Nucl. Phys. B 704 (2005) 3, hep-ph/0409098.
[24] W. Buchmüller, K. Hamaguchi, O. Lebedev, M. Ratz, Nucl. Phys. B 712 (2005) 139, hep-ph/0412318.
[25] W. Buchmüller, K. Hamaguchi, O. Lebedev, M. Ratz, Phys. Rev. Lett. 96 (2006) 121602, hep-ph/0511035.
[26] W. Buchmüller, K. Hamaguchi, O. Lebedev, M. Ratz, Nucl. Phys. B 785 (2007) 149, hep-th/0606187.
[27] W. Buchmüller, K. Hamaguchi, O. Lebedev, M. Ratz, hep-ph/0512326.
[28] W. Buchmüller, C. Lüdeling, J. Schmidt, JHEP 0709 (2007) 113, arXiv: 0707.1651 [hep-ph].
[29] H.P. Nilles, S. Ramos-Sánchez, M. Ratz, P.K.S. Vaudrevange, arXiv: 0806.3905 [hep-th].
[30] O. Lebedev, H.P. Nilles, S. Ramos-Sánchez, M. Ratz, P.K.S. Vaudrevange, Minilandscape II tables, 2008, http://www.th.physik.uni-bonn.de/nilles/Z6IIorbifoldII/.
[31] J. Giedt, Ann. Phys. 289 (2001) 251, hep-th/0009104.
[32] K.R. Dienes, Phys. Rev. D 73 (2006) 106010, hep-th/0602286.
[33] K.R. Dienes, M. Lennek, Phys. Rev. D 75 (2007) 026008, hep-th/0610319.
[34] K.R. Dienes, M. Lennek, D. Senechal, V. Wasnik, Phys. Rev. D 75 (2007) 126005, arXiv: 0704.1320 [hep-th].
[35] H.P. Nilles, Phys. Lett. B 115 (1982) 193.
[36] S. Ferrara, L. Girardello, H.P. Nilles, Phys. Lett. B 125 (1983) 457.
[37] J.P. Derendinger, L.E. Ibáñez, H.P. Nilles, Phys. Lett. B 155 (1985) 65.
[38] M. Dine, R. Rohm, N. Seiberg, E. Witten, Phys. Lett. B 156 (1985) 55.
[39] O. Lebedev, H.P. Nilles, S. Raby, S. Ramos-Sánchez, M. Ratz, P.K.S. Vaudrevange, A. Wingerter, Phys. Rev. Lett. 98 (2007) 181602, hep-th/0611203.
[40] O. Lebedev, H.P. Nilles, S. Raby, S. Ramos-Sánchez, M. Ratz, P.K.S. Vaudrevange, A. Wingerter, Phys. Rev. D 77 (2007) 046013, arXiv: 0708.2691 [hep-th].
[41] W. Buchmüller, J. Schmidt, arXiv: 0807.1046 [hep-th].